Available online at www.sciencedirect.com
SCIENCE DIRECT®
Engineering Fracture Mechanics 71 (2004) 567–577
Engineering Fracture Mechanics
www.elsevier.com/locate/engfracmech

Numerical analysis of indentation fracture in quasi-brittle materials

Alberto Carpinteri, Bernardino Chiaia, Stefano Invernizzi *

Department of Structural Engineering and Geotechnics, Politecnico di Torino, Corso Duca degli Abruzzi 24, 10129 Torino, Italy

Received 30 October 2002; accepted 4 November 2002

Abstract

The process of indentation of brittle and quasi-brittle materials has been investigated both from the experimental and the theoretical point of view. As far as we know, only a few studies have tried to explain the mechanics of cutting due to an indenter which penetrates inside the material. In this paper, an attempt is made to find some general relations for the cutting process in brittle and quasi-brittle materials, under different hypotheses for the microscopic failure behaviour. Fracture patterns in homogeneous brittle solids are obtained by the *finite element method* in the framework of linear elastic fracture mechanics. Microstructural heterogeneities are taken into account by the *lattice model* simulation. Although the reality is often much more complex than the theoretical models applied, the study provides interesting indications for improving performance of cutting tools.

Keywords: Indentation; Cutting; Quasi-brittle fracture

1. Introduction

Many technological operations involve two or more contacting bodies sliding with respect to one another. A series of damage mechanisms can occur in these situations, for instance fretting fatigue and wear. Incommensurable economic losses can be ascribed to these phenomena. In a totally different context, scratching and cutting represent fundamental manufacturing processes, as in the case of cutting precious and ornamental stones or of rock excavations and drilling.

In the framework of plasticity, the *slip-lines theory* was developed to explain the collapse mechanisms of ductile materials under various kinds of contact loading [1]. The process of indentation is completely different in the case of brittle materials [2], and depends also on the shape of the indenter. When brittle materials are loaded by an indenter, three different zones can be distinguished inside the material. Immediately below the wedge, an *hydrostatic core* develops, which is due to the high triaxial compressive stresses induced beneath the indenter. This zone may collapse only by *crushing* and *fragmentation* mechanisms,

* Corresponding author. Tel.: +39-011-5644860; fax: +39-011-5644899.
E-mail address: stefanoinvernizzi@polito.it (S. Invernizzi).

0013-7944/$ - see front matter © 2003 Elsevier Ltd. All rights reserved.
doi:10.1016/S0013-7944(03)00037-7

resembling the effects of strong impacts or explosions. Outside the compressed core, a surrounding zone of large strains develops due to the pushing action of the core. In this area, *tensile cracks* may be initiated starting from pre-existing flaws in the material. Outside this large area (whose size depends on the contact area, on the friction between wedge and base material and on the normal load F_n), the material behaves elastically, and the stress fields predicted by the linear theories can be considered valid.

Fracture patterns in brittle materials, under *blunt indenters*, usually start as ring surface cracks immediately outside the contact area. By increasing the normal load, these surface cracks evolve into the so-called *Hertzian cone cracks*, experimentally revealed by a multitude of tests on glass and other brittle materials (Fig. 1a).

In the presence of *sharp indenters* (e.g. cones or pyramids), the high hydrostatic stresses beneath the tip provide different fracture patterns [3]. In any case, the splitting action of the confined core results in the propagation of an embedded *penny-shaped crack* below the indenter, whose extension is controlled by the size of the hydrostatic core. By increasing the load, the penny-shaped cracks evolve into the *half-penny* configuration, where the crack reaches the surface (Fig. 1a). This was defined as the *median-vent* crack propagation [2].

On the other hand, fracture under tangential loading starts from behind the tool with respect to the cutting direction, where the highest tensile stresses are located (Fig. 1b). Moreover, the fracture pattern depends on the interaction between normal and tangential loads and can evolve into the formation of chips.

Besides the basic patterns described before, other shapes of cracks may develop under indentation, depending on the loading rate, on the density of pre-existing flaws and on the presence of weak planes in the material microstructure.

The effects of material heterogeneity can be very important in the case of the so-called *quasi-brittle materials* (like concrete and many rocks). The role of microstructural disorder is essential because it pro-

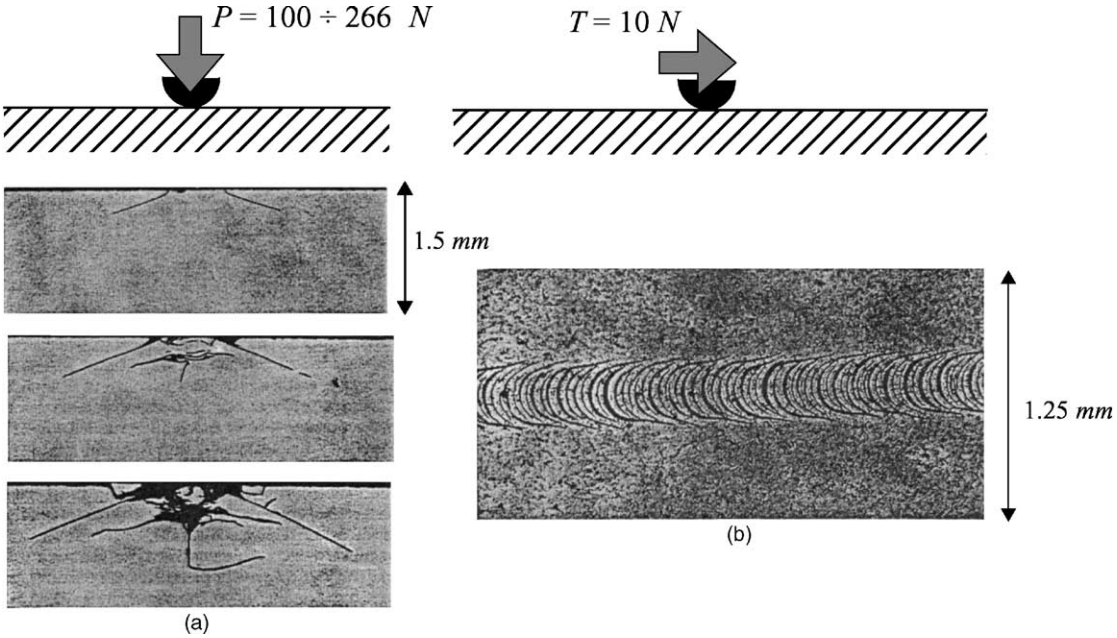

Fig. 1. Experimental crack patterns in soda-lime glass under a blunt rigid indenter [3]. Transition from Hertzian cones to median vent cracks as the normal load is increased (a); chevron-like crack patterns produced by a sliding tungsten carbide sphere (b).

vides a certain amount of 'ductility', which requires an *ad hoc* modelization of the fracture processes. The energy is consumed in the so-called *fracture process zone*, which is a wide zone around the main crack tips, where diffused damage comes into play. The extent of the process zone depends on the material microstructure and also on the size of the indenter.

In the following, the fracture process due to indentation and cutting is numerically simulated both in the case of homogeneous brittle microstructure and of disordered quasi-brittle microstructure. The finite element method (FEM) can be effective for predicting fracture patterns in the homogeneous brittle case, whereas the lattice model (LM) permits to take into account the presence of arbitrary levels of microstructural disorder.

2. Indentation and cutting fracture in homogeneous brittle materials

The FRANC2D software [4], developed at Cornell University, has been used to simulate fracture in the homogeneous case. This software is able to simulate plane-stress, plain-strain as well as axisymmetric crack propagation in the framework of linear elastic fracture mechanics (LEFM). The crack tip is discretized by a *rosette* of isoparametric elements, whereas the stress-intensity factor (SIF) is approximated with the displacement correlation technique (DCT) [5]. The direction of crack propagation, once the critical condition has been reached, can be evaluated both according to the theory of the maximum circumferential stress [6], or to the theory of the minimum strain energy density [7]. The software allows to follow directly the crack propagation thanks to an adaptive re-meshing algorithm running after each propagation step.

For the sake of simplicity, since the code is not able to solve the nonlinear contact problem, both the extent of the contact area and the pressure distribution between the indentor and the elastic half-space are assumed as constant.

2.1. The median vent crack

The problem under consideration is initially axisymmetric. Nevertheless, as soon as the load is sufficiently increased, a bifurcation takes place due to the nucleation of a vertical penny-shaped crack beneath the contact area. Therefore, the exact simulation of the propagation pattern requires a three-dimensional analysis, which is unfortunately beyond the capability of the code. To skip the problem, a simplified plane-strain discretization was adopted, with a linear load distribution in place of the point action.

The median vent crack propagation under a vertical load is shown in Fig. 2a. The initial position of the defect must be carefully assessed. In fact, the defect must be placed at a given depth under the load, in such a way that at least one fracture tip lays outside the hydrostatic compressive core, thus generating a positive SIF. Thus, the crack propagates following a sub-vertical pattern, and no bifurcations are observed.

The SIF has the following general expression:

$$K_{\mathrm{I}} = \sigma\sqrt{a} f\left(\frac{a}{b}\right), \tag{1}$$

where σ is the contact pressure, a the crack length and b the extent of loading area. It is worth noting that the length b is the only characteristic length of this structural scheme. Therefore, in order to emphasize the scale-invarant aspects of the problem, it is useful to plot the diagram of the nondimensional SIF as a function of the crack length normalized with respect to b (Fig. 2b).

After the initial unstable propagation (i.e. SIF increasing with the crack length), fracture becomes stable (i.e. SIF decreasing with the crack length), as soon as the stress field around the tip diminishes.

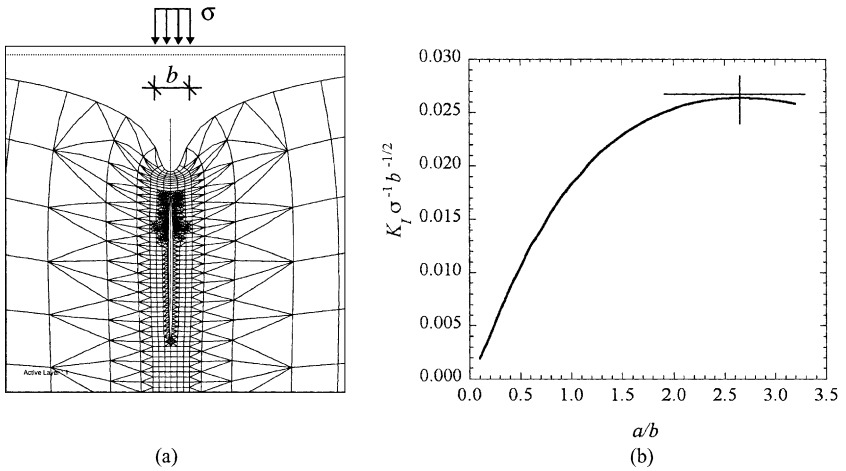

Fig. 2. Deformed *mesh* with FRANC2D: sub-vertical crack propagation under vertical load (a); nondimensional stress-intensity factor as a function of the normalized crack length (b).

2.2. The Hertzian cone crack

In the case of the Hertzian cone crack, fracture starts from the neighborhoods of the contact area, and symmetry is preserved. Therefore, contrary to the previous case, the problem can be modelled with either an axisymmetric or plane-strain discretization resulting in, quite surprisingly, completely different results.

A detailed study of the initial defect position has been carried out, emphasizing that fracture usually initiates from outside the contact area. Although the analysis should be carried out in a probabilistic framework, due to the statistical dispersion of initial flaws in the material, we focused mainly on the deterministic evaluation of the defect position as related to the maximum SIF. As a matter of fact, this is the position of the flaw that is more likely to propagate, in the case of perfectly brittle fracture. In order to take into account the influence of the effective pressure distribution over the contact area, four limit cases have been considered (Fig. 3a,b), which approximate the contact pressure for different indenter profiles. The results are shown in Fig. 3c and d, where the nondimensional SIF of the initial flaw is plotted as a function of its distance normalized with respect to the loaded area. In both cases, and for each pressure distribution, the SIF grows, as the distance increases until a maximum is reached, after which it decreases. This means that the initial flaws which are too close to the contact area (i.e. within the compressive core) cannot propagate, whereas at a certain normalized distance from the load, the probability of propagation is maximum. It is worth noting that this conclusion is in good agreement with the well-known evidence of self-similarity of the fracture cone, observed experimentally both in the quasi-static and in the dynamic case [8].

In the case of the plane-strain analysis (Fig. 3c) the most dangerous defect is placed at a remarkable distance from the loading area, and its position does not depend on the contact pressure distribution. On the contrary, in the axisymmetric case (Fig. 3d), the most dangerous defect lays just outside of the contact area, and gets closer and closer as the contact pressure distribution is decreasing (as in the case of conical indentors).

Once the position of the initial crack was determined, numerical simulations were performed in order to evaluate the geometry and the stability of the crack pattern.

In Fig. 4a the deformed mesh for the plain-strain case is depicted, just after the crack propagation. The diagram of the nondimensional SIF (Fig. 4b) shows a monotonically increasing trend. Therefore, crack propagation is unstable and starts as soon as the critical condition $K_I = K_{IC}$ is reached. In addition, a decreasing tail (softening) should be observed in the load vs displacement diagram, after the peak load.

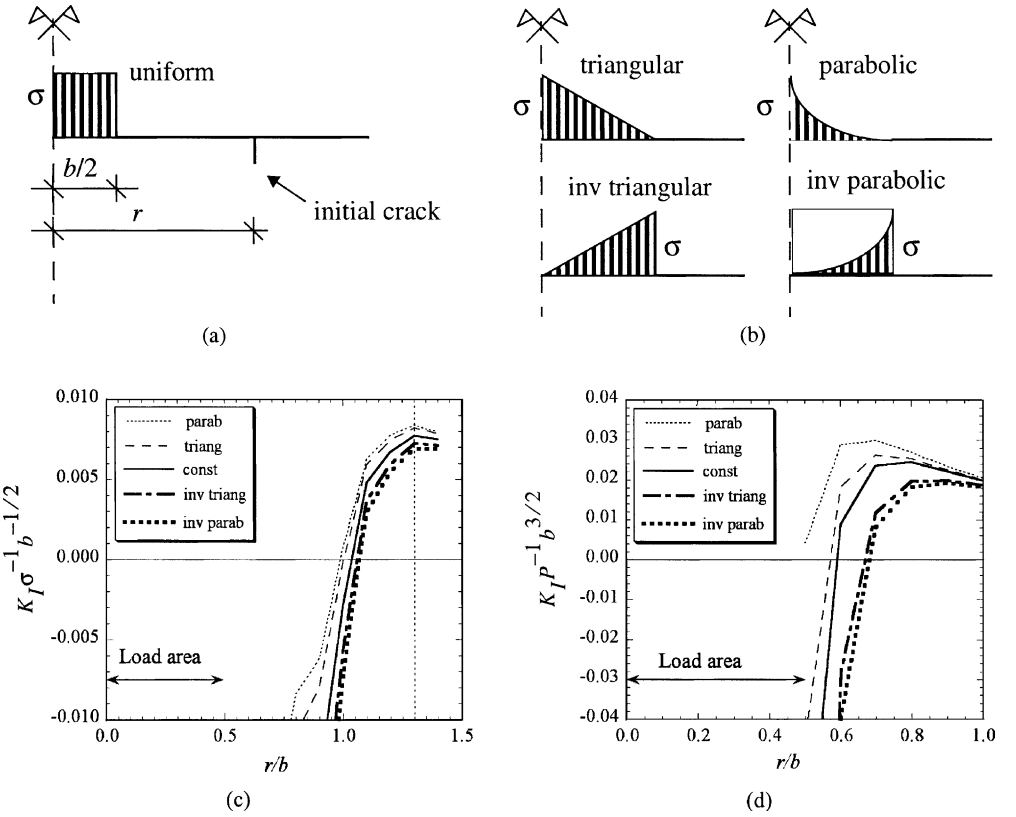

Fig. 3. Structural scheme for the study of the position of the nucleating crack (a); different contact stress distributions considered in the analysis (b); stress-intensity factor as a function of the initial crack position and for different stress distributions: plain-strain analysis (c); axisymmetric analysis (d).

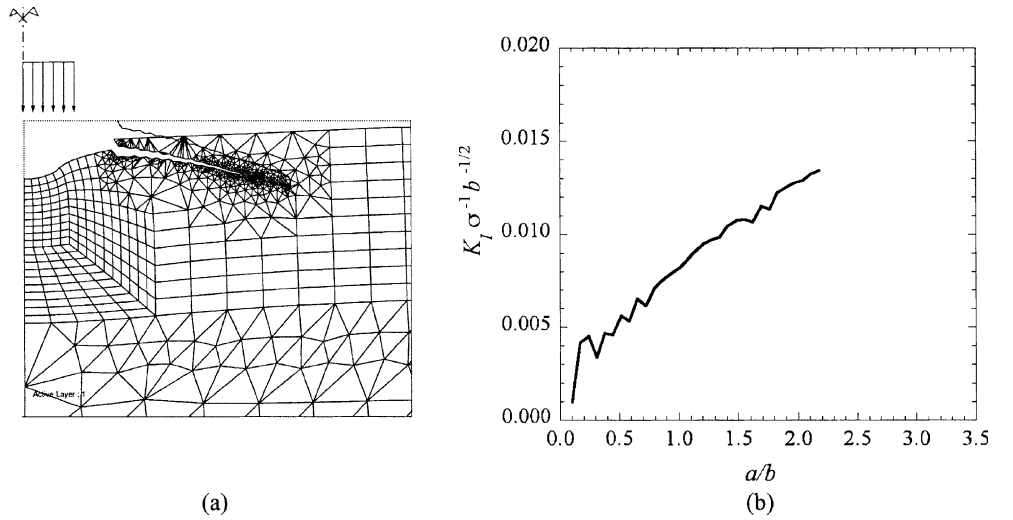

Fig. 4. Deformed mesh with FRANC2D: Hertzian cone crack (a); plain-strain nondimensional stress-intensity factor as a function of the normalized crack length (b).

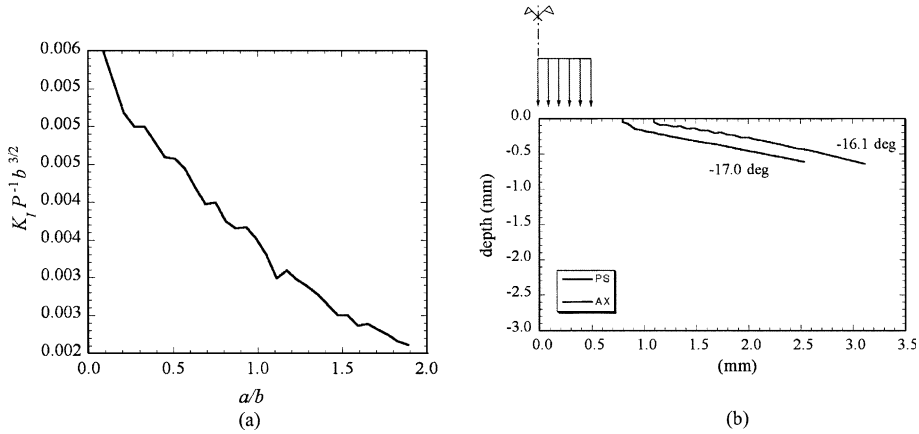

Fig. 5. Axisymmetric nondimensional stress-intensity factor as a function of the normalized crack length (a); comparison between plane-strain and axisymmetric crack patterns (b).

On the other hand, the axisymmetric simulations provide the well-known experimental stable propagation, also recoverable from a theoretical analysis [8]. The SIF history (i.e. the SIF evolution as a function

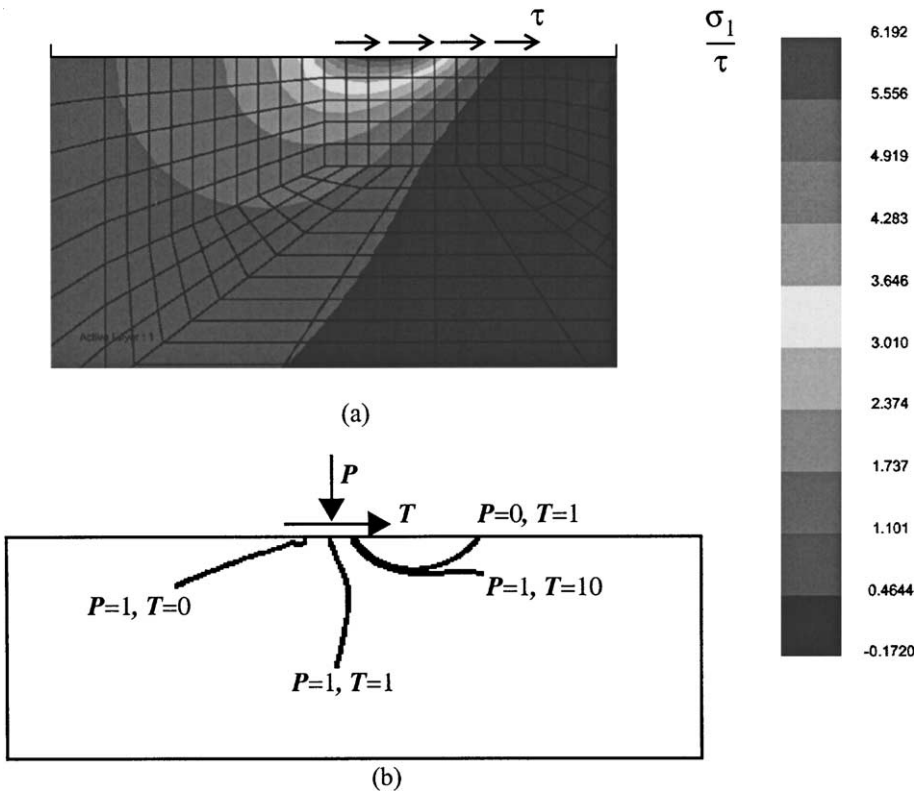

Fig. 6. Principal component of the elastic stress field related to a tangential contact stress distribution (a); different fracture patterns as a function of the normal-tangential load ratio (b).

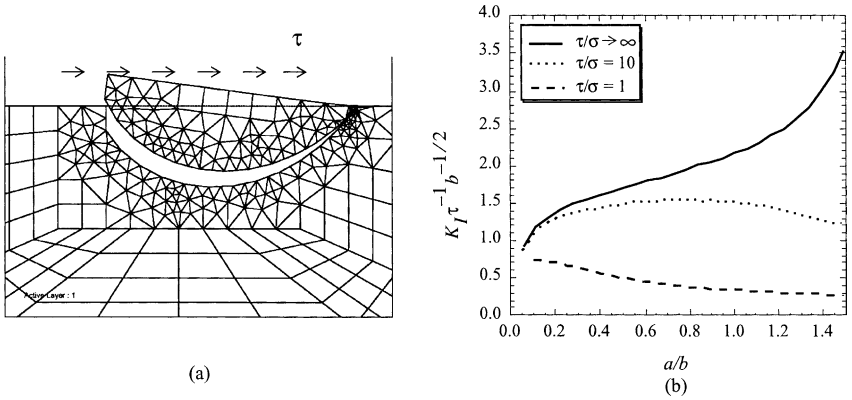

Fig. 7. Deformed FRANC2D mesh related to chip formation (a); normalized stress-intensity factor history (b).

of the crack length), reported in Fig. 5a, is monotonically decreasing. Therefore, an increment of load is necessary after each propagation step and the phenomenon evolves in a stable manner. Finally, in Fig. 5b the crack patterns arising from axisymmetric and plane-strain simulations are compared.

2.3. The cutting crack pattern

A preliminary elastic analysis (Fig. 6a) is useful to put into evidence the zone beneath the loading area, where the crack would preferably nucleate due to the concentration of tensile stresses. In Fig. 6b various cutting patterns are shown for different ratios of the normal and tangential load. As found by other authors [9], when the tangential load prevails, the crack starts from the rear of the contact area (with respect to the tangential load direction), then turns upward (mixed-mode propagation) and provides the formation and removal of a chip (Fig. 7a).

In Fig. 7b a nondimensional diagram is shown where the normalized SIF is plotted as a function of the normalized crack length (i.e. normalized with respect to the contact area). It is thus possible to observe the transition from stable crack propagation (i.e. decreasing SIF) in the case of indentation ($F_n \gg F_t$) to unstable crack propagation in the case of cutting ($F_n \ll F_t$), which is experimentally confirmed by the sudden chip formation detected in brittle materials.

3. Numerical simulation of cutting in heterogeneous materials

In order to investigate the role of heterogeneity in quasi-brittle materials, numerical simulations of indentation by means of the LM [10] have been carried out. The LM is a discrete model of a solid material where the continuum is replaced by an equivalent beam or truss structure, the *lattice*, as shown in Fig. 8. The main purpose of the LM is to achieve understanding of the fracture processes which occur at small scales and of the influence of the microstructural disorder on the global behaviour of the material. A great advantage with respect to the classical codes based on fracture mechanics is that there is no need for an initial crack to be defined. Thereby, we do not need a positive SIF K_I to ensure crack propagation.

Various microstructures have been investigated, by changing the aggregate size distribution, and the ratios between the mechanical properties of the material's phases. In this way, the role of disorder is evidenced.

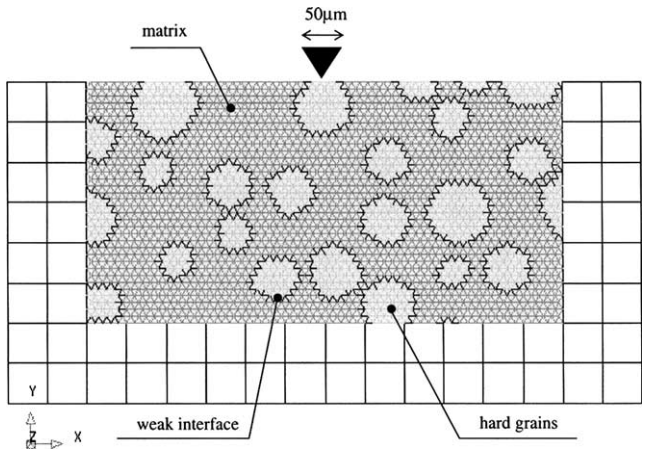

Fig. 8. Three-phases coarse material adopted in the lattice simulations.

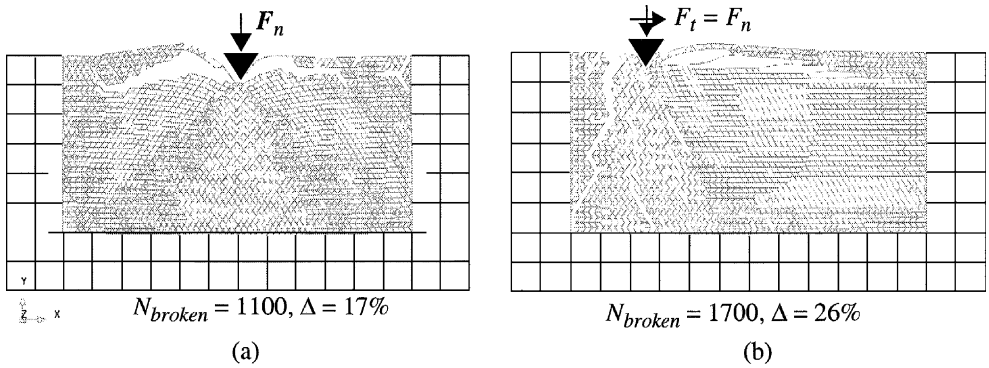

Fig. 9. Evolution of damage in the lattice mesh (coarse material) after increasing the indentation load F_n (a); lattice simulation of the ploughing action in a heterogeneous material (b).

The indentation process can be studied by imposing a vertical displacement to the loaded nodes. The damage level is denoted by the relative number (Δ) of broken bonds (N_{broken}). In Fig. 9a the damage pattern is shown, and the Hertzian cone cracks can be easily recognised as well as the sub-vertical median crack under the indenter.

The action of a ploughing indenter can be simulated by means of the LM, by prescribing vertical and horizontal rigid displacements to the loaded nodes. In Fig. 9b the case of the coarsest microstructure is reported, where $F_t \approx F_n$. Since the cutting force is equal to the normal force, tensile stresses prevail behind the indenter, while a strong compressive field arises ahead of it. As suggested by the elastic stress field, cracks initially develop *behind* the indenter, in the form of vertical splitting fractures. Only when the material becomes significantly weakened in this zone, damage begins to spread inside the compressive field. However, due to the tension-governed fracture law, the LM cannot predict fragmentation within the compressed zone, and only surface delamination is observed in the last stages. Notice, however, the large amount of broken beams (due to the local splitting mechanism in the lattice network) along the maximum compression diagonal direction.

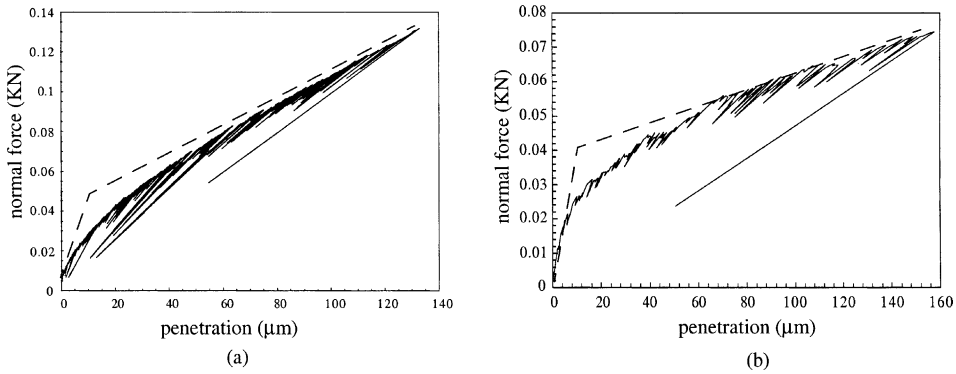

Fig. 10. Numerical load–penetration diagrams for the coarse (a) and the refined (b) microstructures. Notice that the curves are well approximated by a bilinear relation.

Contrarily to the FEM, within the lattice simulation no SIF is provided. Thus a consistent comparison between different microstructures must be carried out in terms of load–penetration responses (Fig. 10), where the greater compliance of coarser microstructure reveals a greater energy dissipation (i.e. ductility) of quasi-brittle microstructures with respect to brittle homogeneous materials.

4. Size effects induced by brittle chipping on cutting strength

In addition to the previous numerical simulations, some theoretical arguments can be put forward regarding the scaling laws involved in the phenomenon. Let us consider two different indenters, pushed inside the base material by different values of the normal force (Fig. 11a,b). Of course, two different values of the cutting force F_t are induced by the two different situations. It is physically plausible to assert that self-similarity holds in the distribution of fragments removed by the ploughing indenters. This similitude is supported by the fractal power-law distributions obtained in several fragmentation and cutting experiments (see the extensive collection of data by Turcotte, [11]). Thereby, assuming the penetration w as the reference length scale, the volume V_f of the removed chip scales as w^3 while the area of the fracture surface A_f scales as w^2.

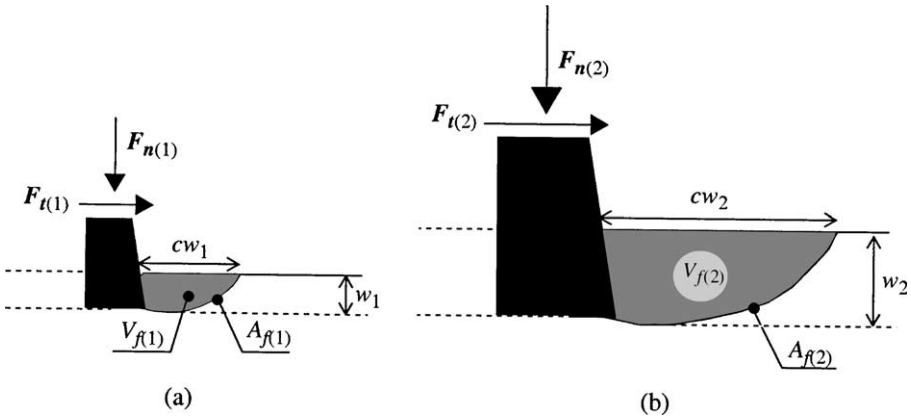

Fig. 11. Geometrical similitude in the discontinuous brittle chipping process.

As is customary in the cutting and drilling practice, the mechanical parameter which defines the material resistance is the cutting strength S which, in the framework of plasticity, has to be considered a scale-independent parameter. Indeed, the cutting process is discontinuous [12]. Thereby, removal of the fragment is governed by LEFM, and the cutting strength undergoes relevant size-effects.

According to LEFM, the failure criterion must be written in terms of the SIF K_I (with physical dimensions $[F][L]^{-3/2}$), to be compared with the fracture toughness of the material, K_{IC}. Thus, the cutting force F_t has to obey the following relation:

$$K_I = \frac{F_t}{w^{3/2}} f = K_{IC}, \tag{3}$$

where f is a nondimensional geometrical function. Dimensional analysis yields, in this case, the following scale dependence of the cutting force on the penetration: $F_t \sim w^{3/2}$. The above scaling law can also be justified by the dimensional disparity inherent to the energy balance. The elastic strain energy stored in the fragment, in fact, scales as w^3 whereas the energy which can be dissipated over the fracture surface scales as w^2. In the case of plastic crushing, instead, both energies would scale as w^3. The intrinsic nonlinearity of chipping (which is independent of the penetration law) implies that a Coulomb-like linear relation is misleading. In fact, in typical cutting experiments [13,14], the ratio F_t/F_n increases with w.

Due to geometrical self-similarity of chips, one can assert that the work W done by the cutting force when removing a single fragment is given by the product of the force times a displacement cw. Therefore, recalling Eq. (3):

$$W_{\text{cutting}} = (F_t \times cw) \propto w^{5/2}, \tag{4}$$

where c is a nondimensional geometrical factor. By definition, the specific work per unit volume is the cutting strength S, with physical dimensions $[J][L]^{-3}$. From Eq. (4) one obtains the following scaling law for the cutting strength:

$$S = \frac{W_{\text{cutting}}}{\kappa w^3} \propto \frac{1}{\sqrt{w}}, \tag{5}$$

where κ is a nondimensional geometrical factor. The scaling law (5), depicted in Fig. 12, is very interesting and is confirmed by the experiments [15]. Therefore, if brittle chipping is the main destructive mechanism, the nominal cutting strength S decreases with the penetration w or, which is equivalent, with the size of the indenter. Bigger indenters will therefore be more efficient cutters, although a larger normal force will be necessary to ensure their penetration. These considerations should be taken in adequate account when performing cutting and drilling operations. Incidentally, it is well-known, in the drilling practice, that larger chip sizes imply a better efficiency (i.e. less energy expenditure). As already mentioned before, the square root scaling should be modified in real situations, because a certain extent of crushing always occurs immediately ahead of the indenter, and thus the two destruction mechanisms interact with each other. In

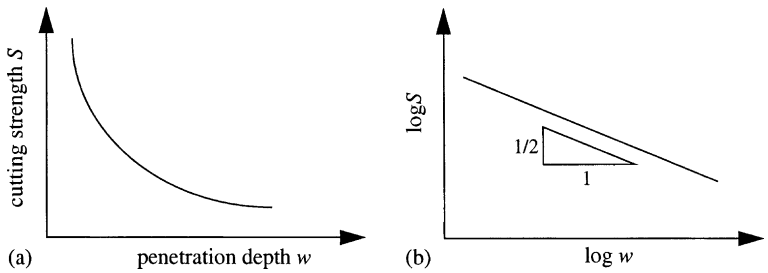

Fig. 12. Size-effects on the cutting strength S according to LEFM (a); corresponding bi-logarithmic diagram (b).

particular, plastic crushing can be very important in some kinds of rocks and even prevail over brittle fracture. Moreover, dynamic effects related to high strain rates can also alter the theoretical predictions.

5. Conclusions

In the present work, the cutting process in brittle and quasi-brittle materials has been simulated. With the help of the LM, the roles of material heterogeneity and diffused damage have been investigated. It has been shown that various mechanisms interact ahead of the indenter during the cutting process (i.e. plastic crushing and brittle chipping). Since the process is discontinuous, some characteristic lengths of damage come into play, related to the indenter's penetration, which provide size-effects on the cutting strength of the material. Theoretical arguments show that the so-called cutting strength S (e.g. energy spent per removed volume of base material) undergoes size-effects. The slope of the curve depends on the interplay of the crushing and brittle chipping mechanisms ahead of the indenter (e.g. if LEFM holds, i.e. very brittle chipping, then $\alpha = 1/2$). Thereby, it can be concluded that the cutting performances could be significantly improved by reducing the crushing component and enhancing the chipping ability of the indenters (e.g. by increasing their sizes or depth of penetration).

Acknowledgements

Support by the Italian Ministry of University and Research (MURST) and by the National Research Council (CNR) is gratefully acknowledged by the authors.

References

[1] Hill R. Mathematical theory of plasticity. Oxford: Clarendon Press; 1950.
[2] Lawn BR, Wilshaw R. Indentation fracture: principles and applications. J Mater Sci 1975;10:1049–81.
[3] Lawn BR, Swain MV. Microfracture beneath point indentations in brittle solids. J Mater Sci 1975;10:113–22.
[4] Bittencourt T, Wawrzynek P, Sousa J, Ingraffea A. Quasi-automatic simulation of crack propagation for 2D LEFM problems. Engng Fract Mech 1996;55:321–34.
[5] Ingraffea AR, Manu C. Stress-intensity factor computation in three dimensions with quarter-point elements. Int J Numer Methods Engng 1980;15:1427–45.
[6] Erdogan F, Sih GC. On the crack extension in plates under plane loading and transverse shear. J Basic Engng 1963;85:519–27.
[7] Sih GC. Strain-energy-density factor applied to mixed-mode crack problems. Int J Fract Mech 1974;10:305–21.
[8] Roesler FC. Indentation hardness of glass as an energy scaling law. Proc Phys Soc London 1955;58:55–60.
[9] Bower AF, Fleck NA. Brittle fracture under a sliding line contact. J Mech Phys Solids 1994;42:1375–96.
[10] van Mier JGM. Fracture Processes of Concrete. Assessment of Material Parameters for Fracture Models. Boca Raton: CRC Press; 1996.
[11] Turcotte DL. Fractals and Chaos in Geology and Geophysics. Cambridge: Cambridge University Press; 1992.
[12] Lopez C, Jimeno E, Lopez F. Drilling and blasting of rocks. Rotterdam: Balkema; 1995.
[13] Mishnaevsky LL. Investigation of the cutting of brittle materials. Int J Mach Tools Manuf 1994;34:499–505.
[14] Mishnaevsky LL. Physical mechanisms of hard rock fragmentation under mechanical loading: a review. Int J Rock Mech Min Sci 1995;32:763–6.
[15] Cook NGW, Hood M, Tsai F. Observations of crack growth in hard rock loaded by an indenter. Int J Rock Mech Min Sci 1984;21:97–107.